A fully self-consistent calculation for positron states: application to aluminium

# A fully self-consistent calculation for positron states: application to aluminium

Xiao-Gang Wang and Hong Zhang

Shanghai Institute of Metallurgy, Academia Sinica, Shanghai 200050, People's Republic of China

**Abstract.** A fully self-consistent scheme based on the two-component density-functional theory and an embedded-cluster model within the framework of the discrete variational method has been developed for calculating positron states in solids. As an example, aluminium is tested. The changes of the electronic structures and positron states for an aluminium vacancy due to the electron–positron interaction are presented. The effects of the atomic relaxations on the positron annihilation characteristics are considered. The results are also compared with former calculations and the conventional scheme.

## 1. Introduction

The positron annihilation technique (PAT) has become a powerful tool for investigation of defects in solids (Hautojärvi 1979, Brandt and Dupasquier 1983). Many calculations on the positron annihilation characteristics of defects in solids have been done in the past few years (Puska and Nieminen 1983, Hansen *et al* 1984, Puska 1987, Puska and Corbel 1988). In solids, the positrons and electrons of which a many-body system is composed move in an ionic potential. The electron–positron interaction changes the electronic structure of the solid. Hence the real positron annihilation characteristics of a defect cannot be directly deduced from its calculated electronic structure in the absence of the positron. It is clear that a fully self-consistent calculation for the system of electrons and positrons is required. The two-component density-functional theory (DFT) (Nieminen 1983, Chakraborty and Siegel 1983) provides the facility needed.

Using the two-component DFT, Nieminen *et al* (1985) and Boroński and Nieminen (1986) calculated the positron annihilation characteristics of vacancies in simple metals, and carefully studied the distorting effect of the localised positron on the electron states in its vicinity and the form of the electron–positron correlation energy and potential as a function of electron and positron densities. In their calculation, the effect of the ion cores of the lattice is neglected, and the vacancy is represented by a spherical hole in a uniform background of positive charge. Their method is inadequate for calculations of positron annihilation characteristics and electronic structures of atomic defects in non-simple metals, alloys and semiconductors. Therefore, new methods for the calculations are needed in which the effects of the ion cores can be included explicitly and which can be used for a wide variety of materials and more complicated defect geometries.

In this paper a fully self-consistent scheme for calculating positron annihilation characteristics is developed, based on the two-component DFT and an embedded-cluster model (Ellis *et al* 1979, Umrigar and Ellis 1980) within the framework of the discrete variational method (Ellis and Painter 1970, Rosén *et al* 1976, Delley and Ellis 1982). Aluminium is chosen as a test case because a lot of relevant experimental data and results of former calculations are available and can be used for comparison with our calculations. The change of the electronic structure and the positron annihilation characteristics of a monovacancy in aluminium due to the electron–positron interaction are presented. The effects of the atomic relaxation around the vacancy of the positron annihilation characteristics are considered. The results are compared with those of former calculations and the conventional scheme in which the electron density is first determined without the influence of the positron and then the positron wavefunction is obtained by solving the Schrödinger equation only once.

## 2. The methods

In the two-component DFT the total energy of the system of interacting electrons and positrons moving in the ionic potential of a solid can be written as a functional of the electron $(n^-)$ and positron $(n^+)$ densities (Nieminen 1983),

$$E[n^-, n^+] = F[n^-] + F[n^+] + \int dr \sum_i \frac{Z_i}{|r - R_i|} [n^+(r) - n^-(r)]$$

$$- \int dr \int dr' \frac{n^-(r)n^+(r')}{|r - r'|} + E_c^{e-p}[n^-, n^+] \tag{1}$$

where $F[n]$ is the one-component functional, $Z_i$ the $i$th ionic charge, $R_i$ the $i$th ionic position and $E_c^{e-p}[n^-, n^+]$ the electron–positron correlation energy functional. Seeking the variational minimum of $E[n^-, n^+]$ with respect to both $n^-$ and $n^+$ leads to a set of one-particle equations for electrons and positrons (in atomic units),

$$-\tfrac{1}{2}\nabla^2 \psi_i^-(r) + \left( \frac{\delta E_{xc}[n^-]}{\delta n^-(r)} + \phi(r) + \frac{\delta E_c^{e-p}[n^-, n^+]}{\delta n^-(r)} \right) \psi_i^-(r) = \varepsilon_i^- \psi_i^-(r) \tag{2}$$

and

$$-\tfrac{1}{2}\nabla^2 \psi_i^+(r) + \left( \frac{\delta E_{xc}[n^+]}{\delta n^+(r)} - \phi(r) + \frac{\delta E_c^{e-p}[n^-, n^+]}{\delta n^+(r)} \right) \psi_i^+(r) = \varepsilon_i^+ \psi_i^+(r) \tag{3}$$

with

$$n^-(r) = \sum_{i(\text{occ})} |\psi_i^-(r)|^2 \qquad n^+(r) = \sum_{i(\text{occ})} |\psi_i^+(r)|^2 \tag{4}$$

where $E_{xc}[n]$ is the exchange–correlation energy functional and $\phi$ the Coulomb potential,

$$\phi(r) = \int dr' \frac{n^-(r') - n^+(r')}{|r - r'|} - \sum_i \frac{Z_i}{|r - R_i|}. \tag{5}$$

In equation (4) the sums go over all the occupied states.

In the local-density approximation (LDA),

$$E_{xc}[n] = \int dr\, n(r)\varepsilon_{xc}(n(r)) \tag{6}$$

and

$$E_c^{e-p}[n^-, n^+] = \int dr\, n^+(r)\varepsilon_c^{e-p}(n^-(r), n^+(r)) \tag{7}$$

where $\varepsilon_{xc}$ is the exchange–correlation energy per particle in a one-component gas (Kohn and Sham 1965), which in the present paper is of the form

$$\varepsilon_{xc}(n(r)) = -\frac{9}{4}\alpha\left(\frac{3}{8\pi}n(r)\right)^{1/3}, \tag{8}$$

where $\alpha$ is the Kohn–Sham–Slater exchange parameter, and $\varepsilon_c^{e-p}(n^-(r), n^+(r))$ is the electron–positron correlation energy per positron, for which in the present paper an interpolation formula furnished by Boroński and Nieminen (1986) is used.

The wavefunctions of electron are expanded in a linear combination of symmetry orbitals $\varphi_j$:

$$\psi_i^-(r) = \sum_j C_{ij}\varphi_j(r) \tag{9}$$

where the $\varphi_j(r)$ are the symmetrised combinations of numerical atomic wavefunctions.

The wavefunctions $\psi_i^+$ of positrons are expanded in a linear combination of Gaussian functions:

$$\psi_i^+(r) = \sum_{j,k}\sum_{l,m,n} C_{lmn}^{jki} X_j^l Y_j^m Z_j^n \exp[-\beta_{lmn}^k(X_j^2 + Y_j^2 + Z_j^2)]. \tag{10}$$

Here $X_j = x - A_j$, $Y_j = y - B_j$, $Z_j = z - D_j$ where $A_j$, $B_j$, $D_j$ are the coordinates of trapping centres of positrons in imperfect solids or the coordinates of the positions of the lowest potential for positrons (generally interstitial positions) in perfect solids, and $\beta_{lmn}^k$ is the Gaussian parameter optimised.

The expansion coefficients $C_{ij}$ and $C_{lmn}^{jki}$ are obtained by solving the secular equation

$$(H - ES)C = 0. \tag{11}$$

The Hamiltonian matrix $H$ and the overlap matrix $S$ are obtained in the discrete variational method as a weighted sum over a set of sample points (Ellis and Painter 1970, Rosén *et al* 1976).

Full self-consistency is obtained as follows. At first, the secular equation of electrons is solved in the situation in which the effect of positrons on the electronic structure is neglected ($n^+ = 0$, conventional scheme), and the electronic eigenvalues, Coulomb potential and electron density $n^-$ are determined. Then the secular equation of positrons is solved and the positron's eigenvalues and positron density $n^+$ are obtained. The $n^-$ and $n^+$ are input to equation (2) and the secular equations of electrons and positrons are again solved in turn; the new $n^-$ and $n^+$ are obtained. The procedure is repeated until self-consistency is obtained.

In the present paper, we have assumed that the wavefunctions of electrons and positrons are centred on a finite cluster of atoms taken from the infinite solid. The rest of the solid manifests its presence by providing a crystal field in which the cluster is

embedded and which can approximately be simulated by the self-consistent potential provided by hundreds of crystal atoms which occupy the lattice sites of several shells of neighbours to the cluster. A one-parameter pseudopotential (Ellis *et al* 1979) is used to truncate exterior wells to prevent electron transfer from the cluster into filled exterior states. Detailed discussions about the embedded-cluster technique have been given by Ellis *et al* (1979) and Umrigar and Ellis (1980).

The positron annihilation rate is proportional to the overlap of electron and positron densities. In the two-component formalism it can be written as

$$\lambda = \pi r_0^2 c \int \mathrm{d}\mathbf{r}\, n^+(r)n^-(r)g\,(0; n^+, n^-) \tag{12}$$

where $r_0$ is the classical electron radius, $c$ the light speed and $g(0; n^+, n^-)$ is the electron–positron pair correlation function evaluated at the positron, which describes enhancement effects in the electron–positron system. An interpolation formula presented by Boroński and Nieminen (1986) for $g(0; n^+, n^-)$ is used in this paper. In the conventional approach, equation (12) becomes

$$\lambda = \pi r_0^2 c \int \mathrm{d}\mathbf{r}\, n^+(r)n^-(r)\Gamma(n^-(r)) \tag{13}$$

where $\Gamma(n^-)$ is the $n^+ \rightarrow 0$ limit of the pair correlation $g(0; n^+, n^-)$ and is called the electron-density enhancement at the positron position, which can approximately take the Brandt–Reinheimer expression (Brandt and Reinheimer 1971)

$$\Gamma(n^-) = 1 + (r_s^3(n^-) + 10)/6 \qquad r_s(n^-) = (3/4\pi n^-)^{1/3}. \tag{14}$$

## 3. Application

We have applied the fully self-consistent scheme to calculate the electronic structures and positron states in aluminium clusters. The perfect Al cluster consisted of 43 atoms including third neighbours of a central atom and having $O_h$ symmetry characteristic of bulk FCC Al, in which the nearest-neighbour Al–Al distance was taken as that in bulk aluminium, namely 5.4094 Bohr. The vacancy was represented by the absence of the central atom in the perfect Al cluster. The external crystal potential was given by 98 atoms, which occupied the lattice sites of five shells of neighbours to the Al cluster. The exchange parameter for electrons was chosen to be 0.72853 (Schwarz 1972).

A positron can interact coulombically with other positrons and electrons but not with itself. In the following calculations, we have only taken into account the case of one positron trapped at a vacancy in the Al cluster. Therefore, in equation (3) we subtracted the positron self-interaction terms

$$\int \mathrm{d}\mathbf{r}'\, \frac{n^+(r')}{|r - r'|} + \frac{\delta E_{xc}[n^+]}{\delta n^+(r)}. \tag{15}$$

The calculations were carried out for the following three cases: (i) the perfect cluster,

**Table 1.** Orbital eigenvalues $\varepsilon$ (Hartree) for aluminium clusters in three cases (see text). The levels are labelled according to the irreducible representations of the $O_h$ point group. Only the occupied levels of the valence electrons are shown.

| Case (i) | | Case (ii) | | Case (iii) | |
|---|---|---|---|---|---|
| Level | $-\varepsilon$ | Level | $-\varepsilon$ | Level | $-\varepsilon$ |
| $13A_{1g}$ | 0.4637 | $11A_{1g}$ | 0.4373 | $11A_{1g}$ | 0.6220 |
| $20T_{1u}$ | 0.4130 | $19T_{1u}$ | 0.4051 | $19T_{1u}$ | 0.5812 |
| $13E_g$ | 0.3617 | $13E_g$ | 0.3598 | $13E_g$ | 0.5286 |
| $15T_{2g}$ | 0.3592 | $15T_{2g}$ | 0.3564 | $15T_{2g}$ | 0.5264 |
| $14A_{1g}$ | 0.3556 | $6A_{2u}$ | 0.3140 | $12A_{1g}$ | 0.4975 |
| $6A_{2u}$ | 0.3133 | $12A_{1g}$ | 0.3129 | $6A_{2u}$ | 0.4819 |
| $21T_{1u}$ | 0.3080 | $20T_{1u}$ | 0.3082 | $20T_{1u}$ | 0.4753 |
| $12T_{2u}$ | 0.2981 | $12T_{2u}$ | 0.2943 | $21T_{1u}$ | 0.4615 |
| $22T_{1u}$ | 0.2971 | $21T_{1u}$ | 0.2804 | $12T_{2u}$ | 0.4606 |
| $16T_{2g}$ | 0.2560 | $16T_{2g}$ | 0.2552 | $16T_{2g}$ | 0.4222 |
| $10T_{1g}$ | 0.2488 | $13A_{1g}$ | 0.2494 | $13A_{1g}$ | 0.4161 |
| $15A_{1g}$ | 0.2481 | $10T_{1g}$ | 0.2487 | $10T_{1g}$ | 0.4141 |
| $17T_{2g}$ | 0.2259 | $14E_g$ | 0.2247 | $17T_{2g}$ | 0.3944 |
| $14E_g$ | 0.2249 | $17T_{2g}$ | 0.2220 | $14E_g$ | 0.3932 |
| $15E_g$ | 0.2189 | $15E_g$ | 0.2159 | $15E_g$ | 0.3843 |
| $16A_{1g}$ | 0.2130 | $7E_u$ | 0.2023 | $7E_u$ | 0.3656 |
| $7E_u$ | 0.2022 | $22T_{1u}$ | 0.1887 | $22T_{1u}$ | 0.3566 |
| $23T_{1u}$ | 0.1907 | $7A_{2u}$ | 0.1848 | $7A_{2u}$ | 0.3505 |
| $7A_{2u}$ | 0.1820 | $23T_{1u}$ | 0.1794 | $23T_{1u}$ | 0.3434 |
| $24T_{1u}$ | 0.1796 | $13T_{2u}$ | 0.1654 | $14A_{1g}$ | 0.3348 |
| $13T_{2u}$ | 0.1661 | $14A_{1g}$ | 0.1598 | $13T_{2u}$ | 0.3285 |
| $25T_{1u}$ | 0.1550 | $24T_{1u}$ | 0.1486 | $24T_{1u}$ | 0.3195 |
| $14T_{2u}$ | 0.1387 | $14T_{2u}$ | 0.1367 | $14T_{2u}$ | 0.3038 |
| $26T_{1u}$ | 0.1358 | $11T_{1g}$ | 0.1305 | $11T_{1g}$ | 0.2943 |
| $11T_{1g}$ | 0.1310 | $18T_{2g}$ | 0.1294 | $18T_{2g}$ | 0.2931 |
| $18T_{2g}$ | 0.1293 | $25T_{1u}$ | 0.1167 | $25T_{1u}$ | 0.2888 |
| $19T_{2g}$ | 0.1105 | $19T_{2g}$ | 0.1119 | $19T_{2g}$ | 0.2771 |

(ii) the cluster with a vacancy and (iii) the cluster with a vacancy and a positron. The occupied orbital eigenvalues and the total density of states (with Lorentzian width parameter 0.015 Hartree) for the clusters are shown, respectively, in table 1 and figure 1. With the multiple-scattering $X_\alpha$ method Iyakutti *et al* (1983) calculated the electronic structures of isolated clusters consisting of only 13 Al atoms, 12 Al atoms plus a vacancy and 12 Al atoms plus a vacancy and a positron. In their calculation, the core orbitals of the atoms were frozen, the effect of the electron–positron correlation on the electronic structure was omitted and the presence of a positron in the cluster was only represented by an extra positive charge. When the presence of a positron is considered in the cluster with a vacancy, in their calculated results the energy levels were shifted up enormously with respect to the vacancy levels; but in our results the levels were pushed down. This difference may be mainly due to whether the core orbitals of the atoms were frozen or not. Indeed, when the 1s, 2s and 2p orbitals of Al atoms were frozen in our calculations, the results showed that the levels were shifted up for the presence of a positron in the cluster with a vacancy. However, the positron lifetimes were insensitive to freezing core orbitals. Freezing 1s, 2s and 2p orbitals only made the positron lifetime at the Al vacancy
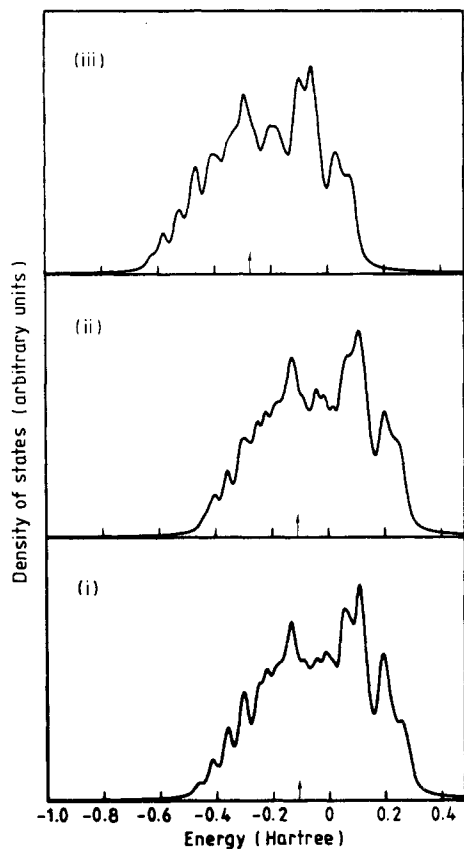
**Figure 1.** Total density of states (with Lorentzian width parameter 0.015 Hartree) for the clusters in cases (i) perfect, (ii) with a vacancy and (iii) with a vacancy and a positron. The arrows indicate the Fermi level.

**Table 2.** Orbital populations for aluminium clusters in the two cases (ii) with a vacancy and (iii) with a vacancy and a positron. (1), (2) and (3) indicate the first-, second- and third-neighbour atoms of the vacancy.

|     | Case (ii) | | | Case (iii) | | |
| --- | --- | --- | --- | --- | --- | --- |
|     | (1) | (2) | (3) | (1) | (2) | (3) |
| 1s  | 2.0000 | 2.0000 | 2.0000 | 2.0000 | 2.0000 | 2.0000 |
| 2s  | 1.9991 | 1.9992 | 1.9993 | 1.9991 | 1.9992 | 1.9993 |
| 2p  | 5.9973 | 5.9978 | 5.9987 | 5.9975 | 5.9978 | 5.9987 |
| 3s  | 1.4221 | 1.3843 | 1.6037 | 1.4574 | 1.3800 | 1.6056 |
| 3p  | 1.4670 | 1.5658 | 1.4688 | 1.5812 | 1.5684 | 1.3923 |

increase 4 ps from 236 to 240 ps and the positron binding energy decrease 0.24 eV from 2.45 to 2.21 eV.

In table 2, the Mulliken orbital populations for the cluster with a vacancy and with a vacancy and a positron are listed, which show the electronic transfer caused by the positron–electron interaction. The electron–positron interaction leads to the increase
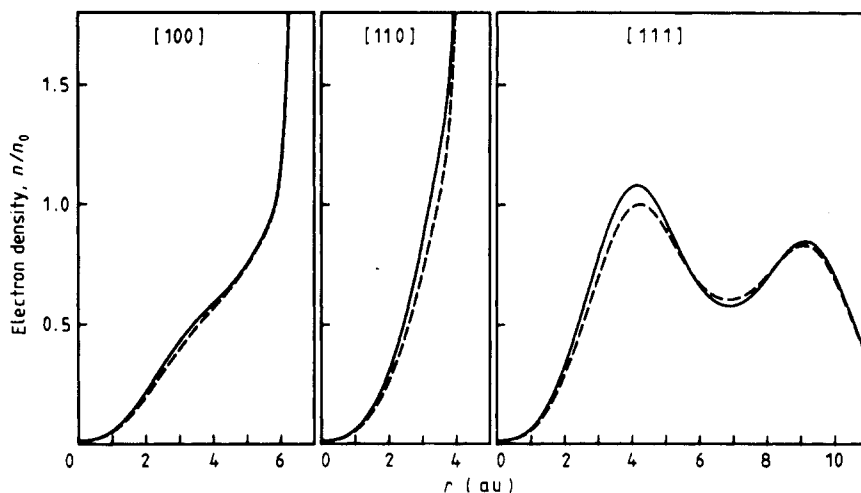
**Figure 2.** Electron density in the Al cluster with a vacancy. Full curves show the result of the two-component DFT scheme; broken curves are for the conventional scheme. The density is given in units of the average electron density $n_0 = 0.027$ au.

of the valence-orbital populations of the first-neighbour atoms of the vacancy. However, the core-orbital populations are not affected by the positron, as seen in table 2.

Figure 2 shows the self-consistent electron density for a vacancy in the cluster with and without a positron present. The increase of electron density at the centre of the vacancy with a positron is only $10^{-4}$ order of magnitude, which is so small that one can hardly see the increase in figure 2. This result is similar to Iyakutti's result (Iyakutti *et al* 1983). However, the calculation of Boroński and Nieminen (1986) showed a large increase of electron density at the centre of the vacancy with a positron. This may be due to the different methods of calculation. In the jellium model, the lattice effects are neglected. In our calculation, owing to the attraction of the ion cores of the lattice, it is difficult for one positron to attract the far electrons into the centre of the vacancy, and near the centre of the vacancy the electron density is very small. Therefore, at the centre of the vacancy the electron density cannot increase largely. In figure 2, one can see the apparent increase away from the centre of the vacancy. A numerical calculation has been done for the change integrated over an $r = 4.8$ (au) spherical space ($r = (X^2 + Y^2 + Z^2)^{1/2}$; the centre of the vacancy is at $X = 0$, $Y = 0$, $Z = 0$). Some 7147 sample points and cubic meshes ($dv = 0.4 \times 0.4 \times 0.4$ (au)) were taken in the space. The change of the charge in the space is 1.099e, which is approximately equal to the total screening charge.

The effective potentials for electrons in both the two-component and the conventional approaches are presented in figure 3. One can see that in the two-component scheme the scattering potential is weaker. This result is in agreement with that of Boroński and Nieminen (1986).

The results for the positron effective potential and the positron density are shown in figure 4. One can see that in the two-component approach the trapping potential for the positron is stronger and the positron is more localised. Table 3 shows that the positron binding energy is larger in the two-component scheme.
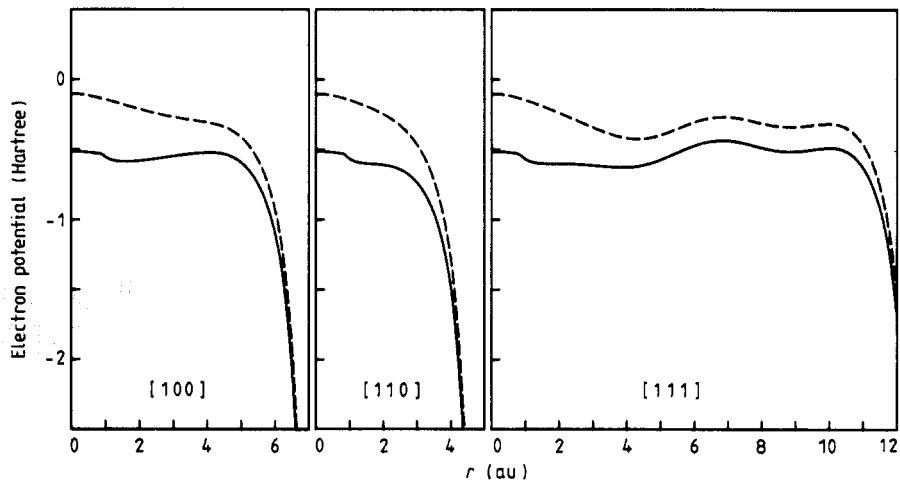
**Figure 3.** Effective scattering potential for electrons in the Al cluster with a vacancy. Full curves show the result of the two-component DFT scheme; broken curves are for the conventional scheme.
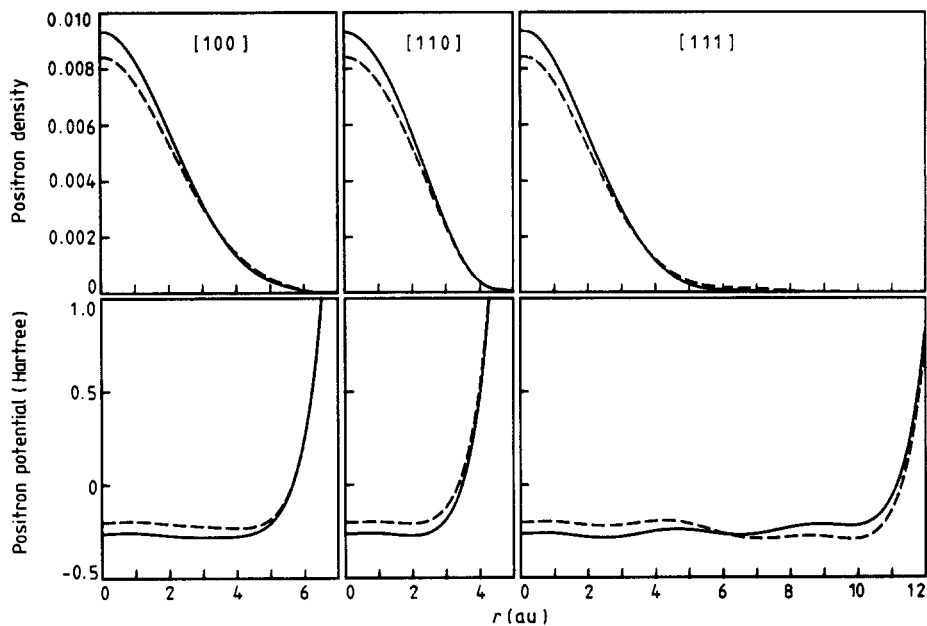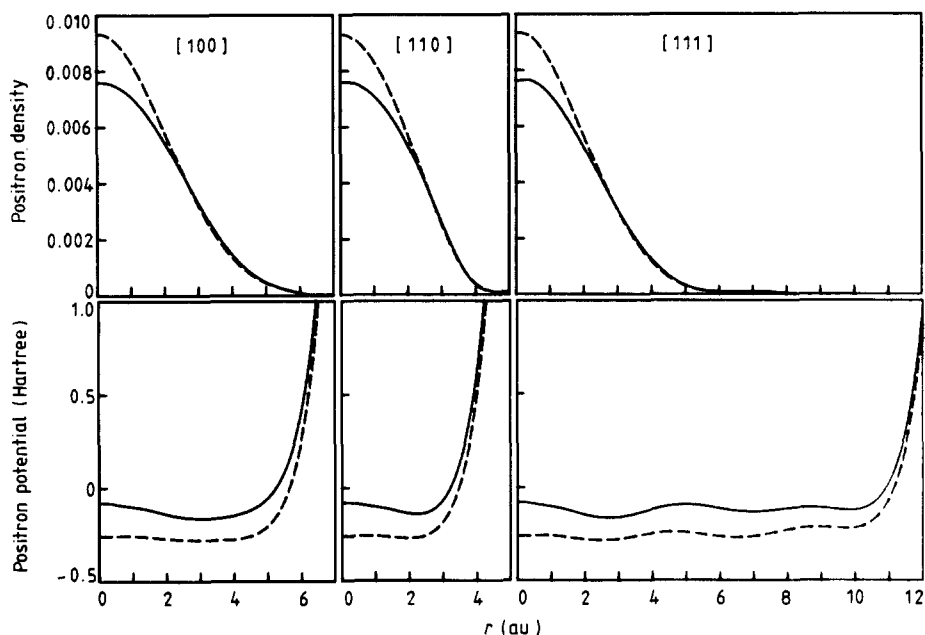


**Figure 4.** Positron effective potential and positron density in the Al cluster with a vacancy. Full curves show the result of the two-component DFT scheme; broken curves are for the conventional scheme.

In the above calculations, the positron self-interaction terms in equation (3) have been omitted. In order to compare our results with those of Boroński and Nieminen (1986), the positron self-interaction terms in equation (3) have been retained in the

**Table 3.** Positron lifetimes and binding energies for Al vacancy. (1) indicates the conventional scheme, (2) the fully self-consistent scheme, which omits the positron self-interaction terms in equation (3), and (3) the fully self-consistent scheme, which retains the positron self-interaction terms in equation (3).

|     | Lifetime (ps) | Binding energy (eV) |
| --- | --- | --- |
| (1) | 244 | 2.11 |
| (2) | 236 | 2.45 |
| (3) | 242 | 1.93 |



**Figure 5.** Positron effective potential and positron density in the Al cluster with a vacancy. Full curves show the result of the two-component DFT scheme including the positron self-interaction terms in equation (3); broken curves are for the two-component DFT scheme not including the positron self-interaction terms in equation (3).

following calculations. For the case of a positron trapped at a vacancy in the Al cluster, the positron self-exchange–correlation potential takes that for a fully spin-polarised system since the single positron has a well defined spin. Figure 5 shows the results for the positron effective potential and the positron density. After adding the positron self-interaction terms in equation (3), the positron binding energy is a little less than that in the conventional scheme and the lifetime becomes larger, as seen in table 3. However, our calculation showed that the change of the electronic structure was small when the positron self-interaction was considered. The calculation gives the positron lifetime $\tau_b =$ 165 ps for bulk aluminium.

**Table 4.** Positron lifetimes and binding energies for Al vacancy with different inward relaxations of 12 nearest-neighbour atoms relative to the vacancy centre. $R$ is the distance from nearest-neighbour atom to the vacancy centre and minus sign denotes inwards relaxation.

| $R$ (%) | Lifetime (ps) | Binding energy (eV) |
|---------|---------------|---------------------|
| −1.00   | 239           | 1.75                |
| −2.00   | 234           | 1.56                |
| −3.00   | 228           | 1.37                |

In table 4 we show the positron lifetimes and binding energies for atomic relaxations. Table 4 shows that the inward relaxations reduce the lifetimes and binding energies, which are sensitive to nearest-neighbour relaxations. The 1% relaxation yields the vacancy lifetime 239 ps, which is in good agreement with the recent experiment (Jackman *et al* 1987).

## 4. Conclusions

The theoretical method presented here for calculating positron annihilation characteristics is of general applicability and can be applied to transition metals, alloys, semiconductors and compounds. This method has the additional advantage of treating atomic relaxations and complicated defect geometries.

The calculations show that the electron–positron interaction changes the electron energy levels and density of state, and causes the electron density and the positron density to be redistributed; however, the positron lifetimes are not sensitive to the calculation methods. Since the fully self-consistent calculations are time-consuming, these are not very necessary only for the determination of the lifetimes, but if more detailed information regarding defects is desired, there seems to be no present alternative to the time-consuming calculations.

## Acknowledgments

## References

Boroński E and Nieminen R M 1986 *Phys. Rev.* B **34** 3820
Brandt W and Dupasquier A (ed) 1983 *Positron Solid State Physics* (*Proc. Int. School Phys. E Fermi LXXXIII*) (Amsterdam: North-Holland)
Brandt W and Reinheimer J 1971 *Phys. Lett.* **35A** 109
Chakraborty B and Siegel R W 1983 *Phys. Rev.* B **27** 4535
Delley B and Ellis D E 1982 *J. Chem. Phys.* **76** 1949

Ellis D E, Benesh G A and Byrom E 1979 *Phys. Rev.* B **20** 1198
Ellis D E and Painter G S 1970 *Phys. Rev.* B **2** 2887
Hansen H E, Nieminen R M and Puska M J 1984 *J. Phys. F: Met. Phys.* **14** 1299
Hautojärvi P (ed) 1979 *Positrons in Solids* (*Topics in Current Physics 12*) (Berlin: Springer)
Iyakutti K, Jean-Louis Calais and Tang Kai A H 1983 *J. Phys. F: Met. Phys.* **13** 1
Jackman J A, Hood G H and Schultz R J 1987 *J. Phys. F: Met. Phys.* **17** 1817
Kohn W and Sham L J 1965 *Phys. Rev.* **140** A1133
Nieminen R M 1983 in Brandt and Dupasquier (1983) p 359
Nieminen R M, Boroński E and Lantto L J 1985 *Phys. Rev.* B **32** 1377
Puska M J 1987 *Phys. Status Solidi* a**102** 11
Puska M J and Corbel C 1988 *Phys. Rev.* B **38** 9874
Puska M J and Nieminen R M 1983 *J. Phys. F: Met. Phys.* **13** 333
Rosén A, Ellis D E, Adachi H and Averill F W 1976 *J. Chem. Phys.* **65** 3629
Schwarz K 1972 *Phys. Rev.* B **5** 2466
Umrigar C and Ellis D E 1980 *Phys. Rev.* B **21** 852